Acoustic properties of oxide glasses at low temperatures

Sonja Rau, Christian Enss, and Siegfried Hunklinger
Institut für Angewandte Physik, Universität Heidelberg, Albert-Ueberle-Strasse 3-5, 69120 Heidelberg, Germany

Peter Neu and Alois Würger
Institut für Theoretische Physik, Universität Heidelberg, Philosophenweg 19, 69120 Heidelberg, Germany
(Received 8 March 1995; revised manuscript received 26 May 1995)

Acoustic properties of a-B_2O_3 and a-GeO_2 are investigated at low frequencies in the temperature range 10 mK $< T <$ 200 K, using a vibrating-reed technique; the results confirm earlier measurements on other amorphous dielectrics. Whereas the low-temperature data are well described by Jäckle's perturbation theory in the framework of the tunneling model, the strong relaxation above 5 K requires a different approach. Up to 20 K incoherent tunneling of two-level systems seems to govern the relaxational dynamics; at still higher temperature the two-level description breaks down, and thermally activated barrier crossing leads to a Arrhenius-like relaxation rate.

I. INTRODUCTION

At low temperature the thermal, acoustic, and dielectric behavior of glasses differs significantly from that of crystalline solids; as examples we note the linear temperature dependence of the specific heat[1] and the most surprising variation of sound velocity with frequency and temperature.[2]

Most experimental observations are well accounted for by the tunneling model[3] which states the existence of almost degenerate configurations for small groups of atoms; these may be simplified to a double-well potential $V(q)$ for some collective coordinate q. For a sufficiently low barrier quantum tunneling permits the atoms moving to and fro between the two configurations.

At low temperature only the ground states $|L\rangle$ and $|R\rangle$ in the two wells are important; with the Pauli matrices $\sigma_z = |L\rangle\langle L| - |R\rangle\langle R|$ and $\sigma_x = |L\rangle\langle R| + |R\rangle\langle L|$, the asymmetry energy Δ and the tunneling amplitude $\Delta_0 = \langle R|V|L\rangle$, the Hamiltonian reads in two-state approximation

$$H_0 = \frac{1}{2}\Delta_0\sigma_x + \frac{1}{2}\Delta\sigma_z. \tag{1.1}$$

According to the tunneling model, its parameters obey the distribution function $P(\Delta_0, \Delta) = \overline{P}/\Delta_0$ with $\overline{P}$ being constant; the ensuing constant distribution for the two-level splitting

$$E = \sqrt{\Delta_0^2 + \Delta^2} \tag{1.2}$$

explains in particular the linear specific heat.

In order to account for the observed relaxation phenomena one needs to consider the coupling of the two-level systems (TLS's) to the thermal motion of the atoms constituting the glass. In linear order in the elastic strain field, the coupling energy reads

$$f = \sum_k (\lambda_k^* b_k + \lambda_k b_k^\dagger), \tag{1.3}$$

here $\lambda_k = -2i\gamma k\sqrt{\hbar/(2m_k\omega_k)}$ where γ is the deformation potential and $k = \omega_k/v$ labels the phonon modes. With (1.1) we obtain the Hamiltonian

$$H = H_0 + \frac{1}{2} f\sigma_z + H_B, \tag{1.4}$$

where $H_B = \sum_k \hbar\omega_k b_k^\dagger b_k$ describes the bath modes whose operators fulfill $[b_k, b_{k'}^\dagger] = \delta_{k,k'}$.

At temperatures below a few K, the dynamics of the two-level systems is only weakly affected by the thermal motion; accordingly one finds coherent oscillations between the states localized in the two wells. Treating the elastic coupling energy $(1/2)f\sigma_z$ as a small perturbation, logarithmic temperature dependence of sound velocity[4,5] and a constant sound attenuation[6] have been derived. Both have been observed for several glasses in the range 100 mK $< T <$ 2 K[2]. This approach, however, fails at very low and at higher temperatures.

For $T <$ 100 mK the attenuation does not vary with T^3 as expected from Jäckle's theory, but rather like T^η with an exponent close to unity; in general the observed attenuation seems to be too large.[7,8] Similar deviations have been reported for the sound velocity.[7] It has been noticed recently that at very low temperature the damping of the two-level systems may be governed by the vibrational amplitude rather than by the elastic distortion;[9] in particular this would explain the excess attenuation and the smaller exponent η.

Above 5 K the sound velocity decreases linearly with temperature[10–12] instead of the logarithmic behavior predicted by theory,[4,5] and the attenuation shows a strong relaxation peak with a maximum at about 30 K.[2,7] In order to explain these deviations, two different scenarios have been proposed, namely (i) the breakdown of the two-level description and (ii) incoherent tunneling arising from overdamped two-level systems.

(i) In the two-state approximation (1.1), phonon scattering occurs between the two ground state levels separated by the energy E (see Fig. 1); perturbation theory yields the one-phonon rate[6]

$$\frac{1}{\tau_{1\mathrm{ph}}} = \frac{1}{2\pi}\frac{\gamma^2}{\varrho v^5\hbar^4}\Delta_0{}^2 E\coth\left(\frac{E}{2k_BT}\right) , \tag{1.5}$$

γ and v are properly averaged over the longitudinal and transverse phonon branch. With rising temperature, excited states in the double-well potential become important and contribute to the damping rate a term of the form const$\times e^{-E_1/k_BT}$ (sometimes referred to as Orbach process), with the excitation energy E_1; under certain circumstances, summing over all higher levels E_1, E_2, $E_3,\ldots$ results for $\Delta \ll T$ in the rate

$$\frac{1}{\tau_{\mathrm{th}}} = \frac{1}{\tau_0}\exp\left(-\frac{V}{k_BT}\right) , \tag{1.6}$$

where $1/\tau_0$ is of the order of the Debye frequency and V is the barrier height between the two wells. In any case, because of its activated behavior, such a rate will at some point exceed the quantum tunneling rate (1.5) which varies only linearly with T.[13–17] (Due to the large prefactor $1/\tau_0$, this crossover will occur at a temperature well below the barrier height V.)

(ii) Damping of tunneling systems in dielectric glasses has been mainly treated using perturbation theory with respect to the elastic coupling energy.[6,4,5] By means of a mode-coupling approximation, finite-order perturbation theory has been shown to break down above a temperature $T^* \propto 1/\gamma$ [see Eq. (2.79) below], resulting in incoherent tunneling motion.[18] Summing all noncrossing diagrams, the characteristic relaxation rate is given by[18,19]

$$\frac{1}{\tau_{\mathrm{MC}}} = \frac{\pi}{2}\sqrt{\frac{\gamma^2 k_B^4}{\varrho v^5\hbar^5}}\,T^2 . \tag{1.7}$$

This picture still relies on the two-state description; yet the thermal motion strongly influences the tunneling dynamics and destroys the phase coherence of quantum oscillations.

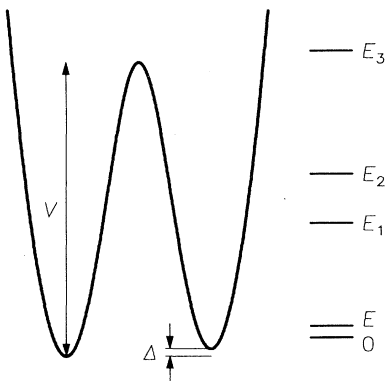

FIG. 1. Schematic representation of an asymmetric double-well potential; in addition the lowest energy levels are indicated with the ground state splitting $E \ll E_1$.

In this paper we discuss acoustic and dielectric properties of amorphous solids for temperatures up to 50 K. Particular attention is given to higher temperatures where we compare experimental data with the theoretical approaches sketched above. A short account of the main results of the mode-coupling approach has been published earlier.[19] The paper is organized as follows.

In the theory part in Sec. II we treat the dissipative dynamics of a two-level tunneling system in the limits of both weak and strong coupling; relying on Mori's projection method and a mode-coupling approximation, we derive novel results for the case of strong coupling or high temperature resulting in the rate (1.7). Then we apply our theory on tunneling systems in glasses and compare with findings obtained earlier for the thermally activated process.

In Sec. III we describe the experimental setup and in Sec. IV we present the experimental results. Section V contains a comparison with theory; in particular we discuss the physical origin of the relaxation peak and the linear sound velocity above 5 K.

II. THEORY

If not otherwise stated, we use units such that $\hbar = 1 = k_B$ in this section. To specify the bath it is convenient to define its spectral density and its spectral function as the Fourier transform of the commutator, respectively, anticommutator of the distortion operator $f(t)$,

$$J(\omega) = \frac{1}{2}\int_{-\infty}^{\infty} e^{i\omega t}\,\frac{1}{2}\langle[f(t),f]_-\rangle_B\,dt \tag{2.1}$$

$$\tilde{J}(\omega) = \frac{1}{2}\int_{-\infty}^{\infty} e^{i\omega t}\,\frac{1}{2}\langle[f(t),f]_+\rangle_B\,dt . \tag{2.2}$$

Here, $[A,B]_\pm = AB \pm BA$ and the average as well as the time evolution is taken with respect to H_B.

In Debye approximation we can rewrite these functions as

$$J(\omega) = \pi\frac{\alpha}{\tilde{\omega}^2}\omega^3\exp(-\omega/\omega_D) , \tag{2.3}$$

$$\tilde{J}(\omega) = J(\omega)\coth(\beta\omega/2) , \tag{2.4}$$

where $\alpha/\tilde{\omega}^2$ is a phenomenological coupling constant containing the deformation potential, the mass density, and the sound velocity; ω_D is the Debye frequency.

In Sec. II A the time evolution of the symmetrized correlation functions

$$\delta G(t) = G(t) - \langle\sigma_z\rangle^2 \tag{2.5}$$

with

$$G(t) = \frac{1}{2}\langle[\sigma_z(t),\sigma_z]_+\rangle \tag{2.6}$$

and

$$C(t) = \frac{1}{2}\langle[\sigma_x(t),\sigma_x]_+\rangle \tag{2.7}$$

are calculated from the equation of motion

$$-i\dot{\sigma}_x = [H,\sigma_x] = i\Delta\sigma_y + if\sigma_y \ , \tag{2.8}$$

$$-i\dot{\sigma}_y = [H,\sigma_y] = i\Delta_0\sigma_z - i\Delta\sigma_x - if\sigma_x \ , \tag{2.9}$$

$$-i\dot{\sigma}_z = [H,\sigma_z] = -i\Delta_0\sigma_y \ . \tag{2.10}$$

Here, $\sigma_i(t) = e^{i\mathcal{L}t}\sigma_i = e^{iHt}\sigma_i e^{-iHt}$ denotes a spin operator in the Heisenberg picture, $\mathcal{L}* = [H,*]$ is the Liouville operator, $\langle\cdots\rangle$ indicates the thermal average with respect to the equilibrium density matrix $\rho_{\rm eq} = \exp(-\beta H)/\mathrm{tr}\exp(-\beta H)$ and $[A,B]_+ = AB + BA$ is the anticommutator. These functions are calculated in the framework of the Mori-Zwanzig projection formalism[20] using a mode-coupling approximation.[21,18]

All experimental information is contained in the corresponding spectral functions

$$G''(\omega) = \frac{1}{2}\int_{-\infty}^{\infty} e^{i\omega t}G(t)dt \ , \tag{2.11}$$

and $C''(\omega)$ defined analogously.

In Sec. II A the TLS dynamics is treated in a perturbative and a mode-coupling approach.

In Sec. II B we review the dynamics beyond the two-level approximation leading to thermally activated relaxation. In Sec. II C the ensemble average over the parameters of the tunneling model is performed and dynamical quantities are derived which can be compared directly with the experimental data.

A. Spin dynamics

We will treat the dynamics of the TLS's in the two asymptotic regimes of coherent tunneling (weak damping) and incoherent tunneling (strong damping) separately. In the coherent regime first-order perturbation theory in the spin-phonon coupling is applicable, whereas the incoherent regime requires a nonperturbative approach. Here we apply a mode-coupling approximation analogously to Refs. 21 and 18. In both regimes we will use the Mori-Zwanzig projection operator formalism. Although a formulation of the dynamics in one projection scheme is possible[22] it turns out convenient to apply different projection schemes for the two asymptotic regimes in the present context.

1. Coherent regime: Perturbation theory

In the low-temperature limit a formulation of the dynamics in the eigenbasis of the spin part of the Liouvillian is most convenient. For this purpose we define the new spin operators

$$\sigma_0 := \frac{\Delta_0}{E}\sigma_x + \frac{\Delta}{E}\sigma_z \ , \tag{2.12}$$

$$\sigma_\pm := \frac{1}{\sqrt{2}}\left(\frac{\Delta_0}{E}\sigma_z - \frac{\Delta}{E}\sigma_x \mp i\sigma_y\right) \ , \tag{2.13}$$

which transform the Hamiltonian into

$$H = \frac{E}{2}\sigma_0 + \frac{1}{2}f\left(\frac{\Delta}{E}\sigma_0 + \frac{1}{\sqrt{2}}\frac{\Delta_0}{E}(\sigma_+ + \sigma_-)\right) + H_B \ . \tag{2.14}$$

In this basis, H is diagonal in the limit of vanishing spin-phonon coupling ($\gamma \to 0$). The operators (2.12) and (2.13) satisfy the commutation relations $[\sigma_0,\sigma_\pm] = \pm 2\sigma_\pm$ and $[\sigma_+,\sigma_-] = \sigma_0$.

In the coherent regime it is most convenient to project the dynamics onto the space spanned by all spin-fluctuation operators ($i = 0,\pm$)

$$\delta\sigma_i = \sigma - \langle\sigma_i\rangle \ . \tag{2.15}$$

These operators span an orthogonal basis

$$(\delta\sigma_i|\delta\sigma_j) \equiv \eta_{ij} = \eta_{ii}\delta_{ij} \tag{2.16}$$

with respect to the scalar product $(A|B) := \frac{1}{2}\langle A^\dagger B + BA^\dagger\rangle$, where due to $\langle\sigma_\pm\rangle = 0$

$$\eta_{00} = 1 - \langle\sigma_0\rangle^2 \ , \tag{2.17}$$

$$\eta_{\pm\pm} = 1 \ . \tag{2.18}$$

With respect to the scalar product $(*|*)$ in Liouville space, the complex correlation matrix ($i,j = 0,\pm$)

$$\delta C_{ij}(z) = i\int_0^\infty e^{izt}\,\delta C_{ij}(t)\,dt \ , \quad \mathrm{Im}\,z > 0 \tag{2.19}$$

of $\delta C_{ij}(t) = (\delta\sigma_i(t)|\delta\sigma_j)$ can be expressed as a resolvent matrix element

$$\delta C_{ij}(z) = \left(\delta\sigma_i\middle|[\mathcal{L}-z]^{-1}\middle|\delta\sigma_j\right) \ . \tag{2.20}$$

Mori's reduction scheme is now performed by defining the projector

$$\mathcal{P} = \sum_{i=0,\pm} |\delta\sigma_i)\eta_{ii}^{-1}(\delta\sigma_i| = \mathcal{I} - \mathcal{Q} \tag{2.21}$$

and applying the resolvent identity onto (2.20)

$$\mathcal{P}\frac{1}{\mathcal{L}-z}\mathcal{P} = \frac{-1}{z - \mathcal{P}\mathcal{L}\mathcal{P} + \mathcal{P}\mathcal{L}\mathcal{Q}\dfrac{1}{\mathcal{Q}\mathcal{L}\mathcal{Q}-z}\mathcal{Q}\mathcal{L}\mathcal{P}}\mathcal{P} \ . \tag{2.22}$$

This yields the matrix equation

$$\delta\mathbf{C}(z) = \eta\frac{-1}{z\eta - \mathbf{\Omega} + \mathbf{M}(z)}\eta \ , \tag{2.23}$$

where the frequency matrix

$$i\Omega_{ij} = \delta\dot{C}_{ij}(t=0) \tag{2.24}$$

contains the free dynamics of the spins, and the memory matrix

$$M_{ij}(t) = (\mathcal{Q}\mathcal{L}\delta\sigma_i|e^{-i\mathcal{Q}\mathcal{L}\mathcal{Q}t}\mathcal{Q}\mathcal{L}\delta\sigma_j) \tag{2.25}$$

the influence of the bath onto the spin dynamics. For the former we obtain

$$\mathbf{\Omega} = \begin{pmatrix} 0 & 0 & 0 \\ 0 & E & 0 \\ 0 & 0 & -E \end{pmatrix} . \tag{2.26}$$

The derivatives appearing in the memory matrix are

easily calculated. Since the operators $\mathcal{QL}\delta\sigma_i$ are already linear in the coupling constants λ_k, the lowest-order Born approximation is achieved by replacing $\mathcal{QLQ}$ with the free spin dynamics $\mathcal{L}_0 = (1/2)E[\sigma_0, *]$ and calculating thermal expectation values with respect to $H_0 := (1/2)E\sigma_0$. Thereby, one finds that the spin and the bath dynamics factorize and that $\langle\sigma_0\rangle = -\tanh(\beta E/2)$ and $\eta_{00} = 1/\cosh^2(\beta E/2)$. With the definition

$$m_i(t) := (\sigma_i(t)f(t)|\sigma_i f)_0 \tag{2.27}$$

the memory function reads, in Born approximation,

$$\mathbf{M}(t) = \begin{pmatrix} 2r(m_+ + m_-) & 0 & 0 \\ 0 & \frac{1}{2}rm_0 + (1-r)m_+ & -\frac{1}{2}rm_0 \\ 0 & -\frac{1}{2}rm_0 & \frac{1}{2}rm_0 + (1-r)m_- \end{pmatrix} , \tag{2.28}$$

where $r \equiv {\Delta_0}^2/E^2$. The Fourier transform of $m_i(t)$ is given by the weighted convolution integral of free spin spectral functions

$$C_{00}^{0\prime\prime}(\omega) = \pi\delta(\omega) , \tag{2.29}$$

$$C_{\pm\pm}^{0\prime\prime}(\omega) = \pi\delta(\omega \mp E) \tag{2.30}$$

with the spectral function of the bath (2.3) and (2.11),

$$m_i''(\omega) = C_{ii}^{0\prime\prime}(\omega) * \tilde{J}(\omega) , \tag{2.31}$$

where we have defined the weighted convolution integral

$$g(\omega) * h(\omega) = \frac{1}{\pi}\int \frac{d\Omega \cosh(\beta\omega/2)}{\cosh(\beta\Omega/2)\ \cosh[\beta(\omega-\Omega)/2]}\, g(\omega-\Omega)\, h(\Omega) . \tag{2.32}$$

This convolution is easily performed; after evaluating the frequency depending memory functions $m_i''(\omega)$ at the poles $\omega = 0, \pm E$, one finds the damping constants

$$\Gamma_1 = \eta_{00}^{-1}\left(rm_+''(0) + rm_-(0)''\right) , \tag{2.33}$$

$$\Gamma_2 = \frac{1}{2}\eta_{\pm\pm}^{-1}\left(rm_0''(E) + (1-r)m_\pm''(\pm E)\right), \tag{2.34}$$

which yield with (2.31)

$$\Gamma_1 \equiv 2\Gamma_2 = r\pi\frac{\alpha}{\widetilde{\omega}^2}E^3\coth(\beta E/2) . \tag{2.35}$$

Using again the transformation (2.12) and (2.13) and calculating the residues of the poles $z_\pm = \pm\widetilde{E} - i\Gamma_2$, $z_0 = -i\Gamma_1$, where $\widetilde{E} = \sqrt{E^2 - \Gamma_2^2}$, up to $O(\Gamma_{1/2}/E)$ one finds for the experimentally relevant spectral function

$$\begin{aligned}\delta G''(\omega) &= G''(\omega) - \pi\langle\sigma_z\rangle^2\delta(\omega) \\ &= \frac{\Delta^2/E^2}{\cosh^2(\beta E/2)}\frac{\Gamma_1}{\omega^2+\Gamma_1^2} + \frac{{\Delta_0}^2/E^2}{2} \\ &\quad\times\left[\frac{\Gamma_2}{(\omega-\widetilde{E})^2+\Gamma_2^2} + \frac{\Gamma_2}{(\omega+\widetilde{E})^2+\Gamma_2^2}\right] ,\end{aligned} \tag{2.36}$$

where

$$\langle\sigma_z\rangle^2 = G(t\to\infty) = \frac{\Delta^2}{E^2}\tanh^2(\beta E/2) . \tag{2.37}$$

Fourier back transformation finally yields

$$\begin{aligned}\delta G(t) &= \frac{\Delta^2/E^2}{\cosh^2(\beta E/2)}e^{-\Gamma_1 t} \\ &\quad + \frac{{\Delta_0}^2}{E^2}e^{-\Gamma_2 t}\cos(\widetilde{E}t-\phi)/\cos(\phi),\end{aligned} \tag{2.38}$$

where $\tan(\phi) = \Gamma_2/\widetilde{E}$.

2. *Incoherent tunneling: Mode-coupling theory*

With increasing temperature the spectral lines of $G''(\omega)$ broaden and move towards the central peak. For the symmetric case $\Delta = 0$ two of the authors have shown that in the frame of a mode-coupling approximation the two inelastic resonances of $G''(\omega)$ merge in one single quasielastic resonance at $(\alpha/\widetilde{\omega}^2)T^2 \approx 1$ whose width narrows with further increasing temperature.[18] This picture remains essentially unchanged in the biased case $\Delta \neq 0$.

In the incoherent regime the dynamics is most easily formulated with the spin operators σ_x, σ_y, and σ_z. Because correlation between different σ_i become less important with increasing temperature, a continued fraction representation of the resolvents

$$G(z) = (\sigma_z|[\mathcal{L}-z]^{-1}|\sigma_z) , \tag{2.39}$$

$$C(z) = (\sigma_x|[\mathcal{L}-z]^{-1}|\sigma_x) , \tag{2.40}$$

is most appropriate for determing the dynamics of (2.6) and (2.7). In the sequel we will repeat the projection procedure for both resolvents up to that point where all memory functions are built by spin-bath operators $f\sigma_i$.

Longitudinal correlation function $C(z)$. Applying Mori's reduction procedure with the projector $\mathcal{P}_x = |\sigma_x)(\sigma_x|$ yields

$$C(z) = \frac{-1}{z+N(z)}, \tag{2.41}$$

with the memory function

$$N(z) = (\mathcal{Q}_x\dot{\sigma}_x|[\mathcal{Q}_x\mathcal{L}-z]^{-1}|\mathcal{Q}_x\dot{\sigma}_x) , \tag{2.42}$$

where

$$\mathcal{Q}_x\dot{\sigma}_x = -\Delta\sigma_y - f\sigma_y . \tag{2.43}$$

Now we separate $N(z)$ into two terms

$$N(z) = \Delta^2 \hat{Y}(z) + N_1(z), \tag{2.44}$$

with

$$\hat{Y}(z) = (\sigma_y|[\mathcal{Q}_x\mathcal{L} - z]^{-1}|\sigma_y) \tag{2.45}$$

and $N_1(z)$ containing the reminder. Repeating the projection for $\hat{Y}(z)$ yields

$$\hat{Y}(z) = \frac{-1}{z + \hat{N}(z)} \tag{2.46}$$

with

$$\hat{N}(z) = (\mathcal{Q}_y\mathcal{Q}_x\dot{\sigma}_y|[\mathcal{Q}_y\mathcal{Q}_x\mathcal{L} - z]^{-1}|\mathcal{Q}_y\mathcal{Q}_x\dot{\sigma}_y)\ , \tag{2.47}$$

$$\mathcal{Q}_y\mathcal{Q}_x\dot{\sigma}_y = f\sigma_x - \Delta_0\sigma_z. \tag{2.48}$$

Splitting off the part arising from $\Delta_0\sigma_z$ provides

$$\hat{N}(z) = {\Delta_0}^2\hat{G}(z) + M_1(z) \tag{2.49}$$

with

$$\hat{G}(z) = (\sigma_z|[\mathcal{Q}_y\mathcal{Q}_x\mathcal{L} - z]^{-1}|\sigma_z)\ , \tag{2.50}$$

as above $M_1(z)$ contains the reminder. Due to $\mathcal{Q}_z\mathcal{Q}_y\mathcal{Q}_x\dot{\sigma}_z = 0$ the correlation function $\hat{G}(z)$ has no dynamics and is therefore given by $\hat{G}(z) = -1/z$.

Thus we have derived a continued fraction representation for the longitudinal correlation function (2.40),

$$C(z) = \cfrac{-1}{z + N_1(z) + \cfrac{-\Delta^2}{z + M_1(z) + \cfrac{-{\Delta_0}^2}{z}}}. \tag{2.51}$$

Transverse correlation function $G(z)$. Proceeding as in the former case yields a similar representation for the transverse correlation function (2.39),

$$G(z) = \cfrac{-1}{z + \cfrac{-{\Delta_0}^2}{z + M_2(z) + \cfrac{-\Delta^2}{z + N_2(z)}}}\ . \tag{2.52}$$

Both continued fractions clearly show the difficulties arising from a finite bias $\Delta \neq 0$. Whereas in the symmetric case $C(z)$ has one pole and $G(z)$ has two poles, here both functions have a three-pole structure. This becomes evident by writing Eqs. (2.51) and (2.52) as

$$C(z) = -\frac{z[z + M_1(z)] - {\Delta_0}^2}{[z + N_1(z)][z^2 + zM_1(z) - {\Delta_0}^2] - z\Delta^2}\ , \tag{2.53}$$

$$G(z) = -\frac{[z + M_2(z)][z + N_2(z)] - \Delta^2}{[z + N_2(z)][z^2 + zM_2(z) - {\Delta_0}^2] - z\Delta^2}\ . \tag{2.54}$$

The memory functions $M_\alpha(z)$ and $N_\alpha(z)$ $(\alpha = 1, 2)$ contain autocorrelations between spin-bath operators $f\sigma_i$, and correlations between spin-bath $f\sigma_i$ and spin operators σ_j furnished with a complicate projected $\mathcal{QL}$ dynamics.

Mode-coupling approximation. The projected $\mathcal{QL}$ dynamics in the memory functions cannot be treated exactly. In a mode-coupling approximation correlation functions of products of operators are decoupled into products of single-operator correlation functions, and the projected $\mathcal{QL}$ dynamics is replaced by the full $\mathcal{L}$ dynamics. Thereby the dynamical equations get closed and the correlation functions can be calculated self-consistently.

In the present case this means

$$M_1(t) = M_2(t) = \frac{1}{2}\Big(\langle\sigma_x(t)\sigma_x\rangle\langle f(t)f\rangle + \langle\sigma_x\sigma_x(t)\rangle\langle f\, f(t)\rangle\Big) \equiv M(t)\ , \tag{2.55}$$

$$N_1(t) = N_2(t) = \frac{1}{2}\Big(\langle\sigma_y(t)\sigma_y\rangle\langle f(t)f\rangle + \langle\sigma_y\sigma_y(t)\rangle\langle f\, f(t)\rangle\Big) \equiv N(t)\ . \tag{2.56}$$

In this approximation mixed correlation functions like $\langle\sigma_i(t)\sigma_j f\rangle$ vanish since the bath operator f appears only linearly.

Using $\partial_t^2\langle\sigma_z(t)\sigma_z\rangle = -{\Delta_0}^2\langle\sigma_y(t)\sigma_y\rangle$ and taking the Fourier transform yields, for the spectral functions,

$$M''(\omega) = [C''(\omega) * \tilde{J}(\omega)]\ , \tag{2.57}$$

$$N''(\omega) = [(\omega/\Delta_0)^2 G''(\omega) * \tilde{J}(\omega)], \tag{2.58}$$

where the convolution product is defined in (2.32). The reactive parts $M'(\omega)$ and $N'(\omega)$ are determined from the spectra $M''(\omega)$ and $N''(\omega)$ via a Kramers-Kronig relation. Together with (2.51) and (2.52), these equations form a closed set of nonlinear, self-consistent equations for $G(z)$ and $C(z)$ or $M(z)$ and $N(z)$. A numerical solution has shown a transition from coherent to incoherent tunneling occuring analogous to the symmetric case.[22,18] To make this transition qualitative we will present below an approximative analytical solution of the mode-coupling equations (2.51), (2.52), (2.57), and (2.58).

Pole approximation. A numerical solution of the mode-coupling equations (2.51), (2.52), (2.57), and (2.58) yields that the spectrum of $G(z)$ consists in the strongly overdamped regime of one single peak centered at $\omega = 0$. The width narrows with increasing temperature and the line shape approaches a Lorentzian form, i.e., the memory functions (2.57) and (2.58) become less frequency dependent. This justifies a pole approximation at $\omega = 0$ in which $M''(\omega)$ and $N''(\omega)$ are set equal,

$$M''(0) = N''(0) \equiv \tilde{\Gamma}. \tag{2.59}$$

In this approximation the reactive parts $M'(\omega)$ and $N'(\omega)$ vanish since they are odd in ω.

The poles of $G(z)$ and $C(z)$ are determined by the complex roots of

$$(z + i\tilde{\Gamma})(z^2 + iz\tilde{\Gamma} - {\Delta_0}^2) - z\Delta^2$$

$$\equiv (z + i\Gamma_1)[(z + i\Gamma_2)^2 - \tilde{E}^2] + R(\tilde{\Gamma}) = 0, \tag{2.60}$$

where we have already used the definitions

$$\Gamma_1 \equiv \frac{{\Delta_0}^2\widetilde{\Gamma}}{E^2+\widetilde{\Gamma}^2}\ , \tag{2.61}$$

$$\Gamma_2 \equiv \widetilde{\Gamma}-\Gamma_1/2\ , \tag{2.62}$$

$$\widetilde{E} \equiv \sqrt{E^2-\Gamma_2^2+(\widetilde{\Gamma}-\Gamma_1)^2}\ , \tag{2.63}$$

$$R(\widetilde{\Gamma}) \equiv {\Delta_0}^2\widetilde{\Gamma}-\Gamma_1\left(E^2+\widetilde{\Gamma}^2+\Gamma_1(\Gamma_1-2\widetilde{\Gamma})\right)\ . \tag{2.64}$$

It is easily seen that $R(\widetilde{\Gamma})$ is negligible in both asymptotic regimes $\widetilde{\Gamma} \ll E$ and $\widetilde{\Gamma} \gg E$. The cubic equation (2.60) is essentially identical to the pole equation for the Ohmic bath in the high-temperature limit.[23] In the present case, however, the width $\widetilde{\Gamma}$ shows quite a different temperature dependence. In the sequel we neglect the term $R(\widetilde{\Gamma})$.

Thus the roots of $G(z)$ and $C(z)$ are approximately given by $z_0=-i\Gamma_1$ and $z_\pm=\pm\widetilde{E}-i\Gamma_2$; in the strongly overdamped regime $\widetilde{\Gamma} \gg E$ we have

$$\Gamma_1 = {\Delta_0}^2/\widetilde{\Gamma}\ , \tag{2.65}$$

$$\Gamma_2 = \widetilde{\Gamma}\ , \tag{2.66}$$

$$\widetilde{E} = \Delta\ . \tag{2.67}$$

In this limit the residue of the damped pole z_0 of $G(z)$ approaches unity whereas the residues of the oscillating poles $z_\pm$ vanish, and vice versa for $C(z)$. Thus we find for $\widetilde{\Gamma} \gg E$ the spectra

$$G''(\omega) \approx \frac{{\Delta_0}^2/\widetilde{\Gamma}}{\omega^2+{\Delta_0}^4/\widetilde{\Gamma}^2}\ , \tag{2.68}$$

$$C''(\omega) \approx \frac{\widetilde{\Gamma}}{\omega^2+\widetilde{\Gamma}^2}, \tag{2.69}$$

which yield the correlation functions

$$G(t) \approx e^{-{\Delta_0}^2 t/\widetilde{\Gamma}}\ , \tag{2.70}$$

$$C(t) \approx e^{-\widetilde{\Gamma}t}\ . \tag{2.71}$$

The temperature dependence of the rate $\widetilde{\Gamma}$ remains to be determined. For this purpose we insert the expression (2.68) for $G''(\omega)$ into (2.58) and evaluate the convolution at $\omega=0$. This yields a self-consistent equation for $\widetilde{\Gamma}$,

$$\widetilde{\Gamma} = \frac{4}{\widetilde{\Gamma}}\frac{\alpha}{\widetilde{\omega}^2}\int_0^\infty \frac{\Omega^5}{\Omega^2+{\Delta_0}^4/\widetilde{\Gamma}^2}\frac{d\Omega}{\sinh(\beta\Omega)}\ . \tag{2.72}$$

Because of $T \gg {\Delta_0}^2/\widetilde{\Gamma}$ we neglect ${\Delta_0}^4/\widetilde{\Gamma}^2$ in the denominator, which permits integration of (2.72),

$$\widetilde{\Gamma} = \frac{\pi^2}{\sqrt{2}}\sqrt{\frac{\alpha}{\widetilde{\omega}^2}}\,T^2\ . \tag{2.73}$$

Inserting (2.69) into (2.57) provides the same expression for $\widetilde{\Gamma}$, thus affirming the consistency of our initial assumption (2.59) and completing the solution of the mode-coupling equations in the incoherent regime.

3. *Relaxation of asymmetric tunneling systems*

In this section we reinsert $\hbar$ and k_B. In the two proceeding sections we have solved the dynamics of an asymmetric TS in the two asymptotic regimes of underdamped and overdamped motion by applying a perturbative and a mode-coupling scheme, respectively. In the intermediate regime where $\widetilde{\Gamma} \approx E$, both approaches are not expected to be valid and no analytical result is available in the present formulation of the dynamics.

However, for all practical purposes this regime is of minor relevance and it may be sufficient to interpolate between the two asymptotic regimes. Since at high temperature $k_BT \gg E$ static spin polarizations $\langle\sigma_i\rangle$ are negligible, we can identify $\delta G(z)$ and $G(z)$ in the incoherent regime. Then the following formulas reasonably interpolate between the behavior in the coherent (2.35), (2.36) and the incoherent regime (2.68), (2.73):

$$\delta G''(\omega) = \frac{\widetilde{\Gamma}^2+\Delta^2/\cosh^2(\beta E/2)}{\widetilde{\Gamma}^2+E^2}\frac{\tau_1}{1+\omega^2\tau_1^2} + \frac{{\Delta_0}^2/2}{\Gamma_2^2+E^2}\sum_\pm \frac{\tau_2}{1+\tau_2^2(\omega\pm\widetilde{E})^2} \tag{2.74}$$

with the relaxation rate ($\Gamma_i=\hbar/\tau_i$)

$$\Gamma_1 = \frac{r\,E^2\,\widetilde{\Gamma}}{\widetilde{\Gamma}^2+E^2} =: \frac{\hbar r}{\tau_{\min}}\ , \tag{2.75}$$

$\tau_{\min}$ being independent of $r \equiv \Delta_0^2/E^2$,

$$\Gamma_2 = \begin{cases} r\widetilde{\Gamma}, & T < T^*, \\ \widetilde{\Gamma}, & T \geq T^*, \end{cases} \tag{2.76}$$

and

$$\widetilde{\Gamma} = \begin{cases} \frac{1}{2\pi}\widetilde{\gamma}^2\,E^3\coth(\beta E/2) =: \widetilde{\Gamma}_{1\mathrm{ph}}, & T < T^*, \\ \frac{\pi}{2}\widetilde{\gamma}\,(k_BT)^2 =: \widetilde{\Gamma}_{\mathrm{MC}}, & T \geq T^*\ . \end{cases} \tag{2.77}$$

Here we have expressed the phenomenological coupling constant $\alpha/\widetilde{\omega}^2$ through the mass density ϱ, the sound velocity v, and the deformation potential[24] γ,

$$2\,\alpha/\widetilde{\omega}^2 \equiv \hbar^2\widetilde{\gamma}^2 = \gamma^2/(\varrho v^5\hbar)\ . \tag{2.78}$$

At the critical temperature T^* the dynamics changes drastically. T^* is defined by $\widetilde{\Gamma}=E$ or, with $E \approx k_BT$, by $\widetilde{\Gamma}_{\mathrm{MC}}(T^*) \equiv k_BT^*$, yielding

$$k_BT^* = \frac{2}{\pi}\frac{1}{\widetilde{\gamma}}\ . \tag{2.79}$$

In an ensemble of TLS's with a wide distribution of level splittings E, this is the temperature where all thermal TLS's ($E \leq k_BT$) are overdamped. This is equivalent to the condition $(\alpha/\widetilde{\omega}^2)T^{*2} \approx 1$ derived previously for the transition to incoherent motion in the symmetric case.[18]

B. Dynamics beyond the two-level approximation

With increasing temperature, the occupation of excited levels in each well can no longer be neglected and tunneling from these levels may occur. If there are sufficiently many levels below the top of the barrier, this results in an effective activation energy V. The rate of thermally activated barrier crossing reads

$$\tau_{\rm th}^{-1} = \tau_0^{-1} \exp\left(-\frac{V}{k_B T}\right) \cosh\left(\frac{\Delta}{2k_B T}\right) . \quad (2.80)$$

Since the seminal work of Kramers,[25] there has been much progress on the understanding of the transition between the tunneling and the thermal activated regime (for a review see Refs. 26 and 27). These works are mainly concerned with a modification of the preexponential factor, the so-called attempt frequency τ_0^{-1}. However, with respect to the ensemble average to be performed later, the attempt frequency only contributes logarithmically and the mentioned modification play no essential role in glasses. Thus, we may safely treat τ_0^{-1} as a constant which is of the order of the Debye frequency.

C. Tunneling systems in glasses

In glasses one finds an ensemble of tunneling systems (TS's) with a wide distribution of parameters Δ_0 and Δ. In order to compare our calculation with experiments, an ensemble average over all TS's has to be performed. Here we will stay in the framework of the standard tunneling model[3] and apply the distribution function $P(\Delta_0, \Delta) = \overline{P}/\Delta_0$ for the parameters Δ_0 and Δ, which is equivalent to

$$P(E, r)\, dE\, dr = \frac{\overline{P}}{2r\sqrt{1-r}}\, dE\, dr \quad (2.81)$$

with a constant $\overline{P}$ and $r = {\Delta_0}^2/E^2$, where $r_{\rm min} \le r \le 1$. The resulting wide distribution of the two-level splitting E and relaxation times are the main assumption of the tunneling model. In the following we will always assume that the upper bound $E_{\rm max}$ is much larger than all other energies; thus we set $E_{\rm max}$ equal to infinity. The logarithmic divergence of the integral $\int dr P(E, r)$ requires a finite lower cutoff $r_{\rm min}$. Macroscopic quantities are obtained by the average

$$\overline{\mathcal{O}} = \int_0^{E_{\rm max}} dE \int_{r_{\rm min}}^1 dr\, P(E, r)\, \mathcal{O} . \quad (2.82)$$

An equivalent description of the low-temperature properties of glasses is given by the soft potential model[14] (SPM) (for a review see Ref. 17). There, the local potential of the tunneling defect as shown in Fig. 1 is parametrized. In comparison to the tunneling model, this leads to a slightly different distribution function $P(E, r)$ of the tunneling parameters. In addition to the double-well potentials, soft harmonic potentials may also exist in glasses according to this description. With these localized quasiharmonic modes, universal properties of glasses at higher temperatures (above ~ 1 K), like the plateau in the thermal conductivity[15] and the bump in the specific heat,[16] are qualitatively accounted for. At lower temperatures, the SPM yields the same results as the tunneling model in the coherent regime.

An external field $h_{\rm ext}(t)$ couples to the operator σ_z only, resulting in an additional term $\sigma_z h_{\rm ext}(t)$ in the Hamiltonian. For not too strong an interaction, linear-response theory with respect to $h_{\rm ext}(t)$ is applicable so that any experimental quantity may be expressed in terms of the symmetrized transverse correlation spectrum $\delta G''(\omega)$. It is related to the dynamical susceptibility

$$\chi(z) = \frac{i}{\hbar} \int_0^\infty e^{izt} \langle [\sigma_z(t), \sigma_z]_- \rangle dt \quad (2.83)$$

by a fluctuation-dissipation theorem (FDT),

$$\chi''(\omega) = \frac{2}{\hbar} \tanh(\beta\hbar\omega/2)\, \delta G''(\omega) , \quad (2.84)$$

where $\chi(z = \omega + i0^+) = \chi'(\omega) + i\chi''(\omega)$.

Experimentally accessible quantities, like internal friction and variation of sound velocity follow from this via[2]

$$Q^{-1} = \frac{\gamma^2}{\varrho v^2}\, \overline{\chi''(\omega)} , \quad (2.85)$$

$$\frac{\delta v}{v} = -\frac{1}{2}\, \frac{\gamma^2}{\varrho v^2}\, \overline{\chi'(\omega)} . \quad (2.86)$$

For low-frequency acoustic experiments on glasses, the temperature always exceeds the applied frequency, $\hbar\omega \ll k_B T$. Then, resonant processes are strongly suppressed and will be neglected hereafter. In this regime, we may replace $\tanh(\beta\hbar\omega/2) \approx \beta\omega/2$ in the FDT which yields, together with the Kramers-Kronig relation,

$$\chi''(\omega) = \beta\omega\, \delta G''(\omega) , \quad (2.87)$$

$$\chi'(\omega) = \beta/\tau_1\, \delta G''(\omega) . \quad (2.88)$$

The relaxation process of biased TS's has been elaborated by Jäckle[6] using Fermi's Golden Rule. Then the relaxation rates are given by the one-phonon expression (2.35) and the dynamics is governed by coherent tunnelling, cf. Eq. (2.36).

The relaxation of overdamped TS's has not been considered so far. Commonly, it was assumed that thermally activated relaxation is responsible for the experimentally observed deviation above 5 K from the prediction of the tunneling model. This has been worked out in detail by Tielbürger *et al.*,[13] and within the SPM by Buchenau *et al.*[15]

Before we summarize this theory in Sec. II C 2, let us show, how far we can get within the two-level approximation by including the incoherent tunneling regime.

1. *Dynamics of two-level tunneling systems in glasses*

Here we assume that the two-level approximation is valid beyond 5 K; as an essential result we note that the strong rise of the absorption and the linear decrease of

the sound velocity found above ~ 5 K may be attributed to relaxation via incoherent tunneling.

We have to perform the ensemble average over all TS's whose dynamics is given by the results of Sec. II A. In expression (2.74) for $\delta G''(\omega)$ only the relaxational pole at $\omega = 0$ is relevant. With this and Eqs. (2.81), (2.82), (2.85), and (2.86) and the relations for the rates of Sec. II A 3 one finds

$$Q^{-1} = \frac{C}{2k_BT} \int \frac{dE}{\widetilde{\Gamma}^2 + E^2} \int_{r_{\min}}^{1} dr \left(\frac{\widetilde{\Gamma}^2}{\sqrt{1-r}} + \frac{E^2\sqrt{1-r}}{\cosh^2(\beta E/2)} \right) \frac{\omega\tau_{\min}}{r^2 + \omega^2\tau_{\min}^2} , \tag{2.89}$$

$$\frac{\delta v}{v} = -\frac{C}{4k_BT} \int \frac{dE}{\widetilde{\Gamma}^2 + E^2} \int_{r_{\min}}^{1} dr \left(\frac{\widetilde{\Gamma}^2}{\sqrt{1-r}} + \frac{E^2\sqrt{1-r}}{\cosh^2(\beta E/2)} \right) \frac{r}{r^2 + \omega^2\tau_{\min}^2} , \tag{2.90}$$

where we have defined the dimensionless constant

$$C = \frac{\overline{P}\gamma^2}{\varrho v^2} . \tag{2.91}$$

An analytical evaluation of the integrals is possible in the limits $\omega\tau_{\min} \gg 1$ and $\omega\tau_{\min} \ll 1$. This defines the temperature $\widetilde{T}$ via the condition $\omega\tau_{\min} = 1$. Provided that the one-phonon process dominates at low temperatures this yields, after substituting $E = k_BT$ [cf. Eqs. (2.75) and (2.77)],

$$k_B\widetilde{T} = \left(\frac{\omega\pi}{\widetilde{\gamma}^2} \right)^{1/3} . \tag{2.92}$$

One finds for the internal friction by cutting the E-integration at $E = \max(k_BT, \widetilde{\Gamma})$

$$Q^{-1} = \begin{cases} \pi^3 C \widetilde{\gamma}^2 k_B^3 T^3/(24\hbar\omega), & T < \widetilde{T}, \\ \frac{\pi}{2} C \left[1 - \frac{\widetilde{\Gamma}_{MC}}{2k_BT} \arctan\left(\frac{2k_BT}{\widetilde{\Gamma}_{MC}} \right) \right], & \\ + \frac{\pi}{2} C \frac{\widetilde{\Gamma}_{MC}}{2k_BT} \left[\frac{\pi}{2} - \arctan\left(\frac{\widetilde{\Gamma}_{MC} r_{\min}}{\hbar\omega} \right) \right], & T > \widetilde{T} . \end{cases} \tag{2.93}$$

$\widetilde{\Gamma}_{MC}$ is defined in (2.77). At very low temperature $T < \widetilde{T}$ (corresponding to $\omega\tau_{\min} \gg 1$), relaxation attenuation increases with T^3; in the range $T > \widetilde{T}$ we distinguish three different laws,

$$Q^{-1} = \begin{cases} \frac{\pi}{2} C, & \widetilde{T} < T < T^*, \\ \frac{\pi^2}{8} \frac{T}{T^*}, & T^* < T < T_{\max}, \\ \frac{\pi C}{4r_{\min}} \frac{\hbar\omega}{k_BT}, & T > T_{\max}. \end{cases} \tag{2.94}$$

The temperature $T_{\max}$ where the maximum in the absorption occurs is obtained from the relation $\hbar\omega = r_{\min}\widetilde{\Gamma}_{MC}$ [cf. Eq. (2.93)] which yields

$$k_BT_{\max} = \sqrt{\frac{2\hbar\omega}{\pi\widetilde{\gamma}r_{\min}}} , \tag{2.95}$$

i.e., the maximum temperature varies as $T_{\max} \propto \sqrt{\omega}$.

The three characteristic temperatures $\widetilde{T}$, T^*, and $T_{\max}$, and the typical line shape of the internal friction are schematically illustrated in Fig. 2.

After adding the contribution of the resonant part $\delta v/v|_{res} = C\ln(T/T_0)$ to Eq. (2.90) one finds for the change of the sound velocity

$$\frac{\delta v}{v} = \begin{cases} C \ln\frac{T}{T_0}, & T < \widetilde{T}, \\ -\frac{1}{2} C \ln\frac{T}{T_0}, & \widetilde{T} < T < T^*, \\ -(\frac{1}{4} + \frac{\pi}{16}) C \frac{T}{T^*} \ln\left(\frac{k_BT^2}{T^*\hbar\omega} \right), & T > T^* . \end{cases} \tag{2.96}$$

Both the increase with T^3 and the plateau value $\pi C/2$ of the internal friction[6] and the logarithmic temperature dependence of the sound velocity[4,5] have been derived more than 20 years ago. Below $\widetilde{T}$ even the fastest TS's (i.e., the symmetric TS) are too slow to contribute to relaxation, so that for $T < \widetilde{T}$ the resonant interaction prevails. Below T^* one finds the well-known logarithmic temperature dependence of the sound velocity and the constant internal friction. At $T = T^*$ the temperature dependence changes to a linear increase in the absorption and a linear decrease in the sound velocity.

2. *Activated relaxation in glasses*

Here we summarize the theory of Tielbürger *et al.*[13] on thermal activated relaxation in glasses (see also Ref.

15 for a description within the SPM). In these works it is assumed that the two-level description breaks down before the tunneling dynamics changes from coherent to incoherent motion. As a result, the relaxation peak is attributed to thermally activated relaxation instead of incoherent tunneling.

The expressions for the internal friction and the sound velocity read[13]

$$Q^{-1} = \frac{\beta\gamma^2}{\varrho v^2} \int_0^\infty \int_0^\infty d\Delta_0\, d\Delta\, P(\Delta_0, \Delta) \left(\frac{\Delta^2/E^2}{\cosh^2(\beta E/2)} \right) \frac{\omega\tau_{\rm th}}{1+\omega^2\tau_{\rm th}^2}, \tag{2.97}$$

$$\frac{\delta v}{v} = -\frac{\beta\gamma^2}{2\varrho v^2} \int_0^\infty \int_0^\infty d\Delta_0\, d\Delta\, P(\Delta_0, \Delta) \left(\frac{\Delta^2/E^2}{\cosh^2(\beta E/2)} \right) \frac{1}{1+\omega^2\tau_{\rm th}^2} . \tag{2.98}$$

Since the thermal rate $\tau_{\rm th}^{-1}$ (2.80) depends on the barrier height V, the distribution function $P(\Delta_0, \Delta)$ must be transformed to $P(\Delta, V)$. Most simply, one assumes the WKB expression for the tunneling frequency

$$\Delta_0 \approx \frac{2E_0}{\pi} e^{-\lambda} , \tag{2.99}$$

with tunneling parameter $\lambda = (d/2\hbar)\sqrt{2mV}$. Here, E_0 represents the zero-point energy, m the mass of the tunneling unit, and d the distance between the minima of the double-well potential. Assuming the double well to consist of two harmonic potentials, we have $V \propto d^2$ and

$$\lambda = \frac{V}{E_0}. \tag{2.100}$$

From this one deduces the uniform distribution

$$P(\Delta, V) = \frac{\overline{P}}{E_0} \tag{2.101}$$

up to a cutoff $V_{\rm max}$. As a smooth physical cutoff, Tielbürger *et al.* have proposed a Gaussian distribution with width σ_0,[13]

$$P(\Delta, V) = \frac{\overline{P}}{E_0} \exp\left(-V^2/2\sigma_0^2\right) . \tag{2.102}$$

For barriers V being relevant for relaxational absorption, $V \ll \sigma_0$, Eqs. (2.101) and (2.102) are equivalent. Using the uniform distribution function (2.101) and putting $\Delta \approx E \approx k_B T$, the integrals in (2.97) and (2.98) are easily evaluated and one finds[13]

$$Q^{-1} = \frac{\pi C k_B T}{E_0} \equiv \frac{\pi}{2} \frac{T}{T_a} , \tag{2.103}$$

$$\frac{\delta v}{v} = \frac{C k_B T}{E_0} \ln(\omega\tau_0) , \tag{2.104}$$

for $\omega\tau_0 \ll 1$. Thus, again, the absorption increases linearly, and the sound velocity decreases linearly above $T_a \approx 5$ K. Comparing these expressions with Eqs. (2.94) and (2.96), one sees that additional parameters E_0 and τ_0 have been introduced.

From the relation $\omega\tau_{\rm th} = 1$ one expects the maximum in the absorption to occur at

$$k_B T_{\rm max} = -\frac{V_{\rm max}}{\ln(\omega\tau_0)} , \tag{2.105}$$

i.e., the maximum temperature varies with frequency as $T_{\rm max} \propto \ln(\omega)$.

A word of caution is in order concerning the link between the tunneling amplitude and activation energy, Eqs. (2.99)–(2.102). At 5 K only low barriers contribute to relaxation; thus one may doubt whether the activated behavior really reflects classical activated barrier crossing or whether it is rather due to tunneling at higher levels (e.g., between E_1 and E_2 in Fig. 1). In the latter case the distribution of activation energies would be different from (2.102).

Finally we compare with the results obtained from the soft-potential model. Due to the slightly modified distribution function, the SPM (Ref. 15) leads to $Q_{\rm TS}^{-1} \propto T^{3/4}$ and accordingly $(\delta v/v)_{\rm TS} \propto -T^{3/4}$. The experimentally observed linear decrease of $\delta v/v$ arises in the SPM only from the contribution of soft harmonic oscillators[17] $(\delta v/v)_{\rm HO} \propto -T$.

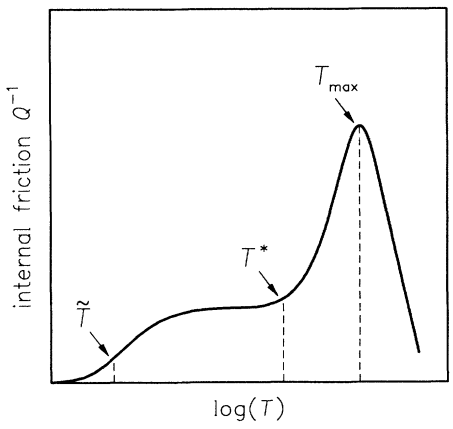

FIG. 2. Typical line shape of the internal friction Q^{-1} where the different characteristic temperatures $\widetilde{T}$ [cf. Eq. (2.92)], T^* [cf. Eq. (2.79)], and $T_{\rm max}$ [cf. Eq. (2.95)] are indicated. For thermally activated relaxation processes, T^* has to be replaced by T_a.

III. EXPERIMENTAL SETUP

Relative sound velocity $\delta v/v$ and internal friction measurements Q^{-1} were performed using the vibrating reed technique.[28] The basic idea of this technique is to determine the resonance frequency and the amplitude of a small rectangular plate which is clamped on one end and which is driven electrostatically to forced vibrations on its free end. In our experiment the samples were about 0.2 mm thick, 3 mm wide, and 10–15 mm long. They were clamped between two copper blocks to ensure good thermal contact. The sample holder was attached to the mixing chamber of a ^{3}He/^{4}He dilution refrigerator providing temperatures down to 8 mK. The samples were covered with a 30–50 nm sputtered gold layer, which served as a counter electrode for both the driving and detection voltage. This gold layer is thin enough to exclude any noticeable influence on our measured quantities.

Figure 3 shows a schematic of the electrical circuit used to keep the driving force at the resonance frequency of the reed. The periodical driving voltage U_d is produced by a synthesized generator (Philips PM 5191). Due to the quadratic relation between the applied voltage and acting force F the reed vibrates with twice the driving frequency f. The resulting amplitude is detected by a two-phase lock-in amplifier. Using the lock-in output signal $A\cos(\phi)$ the synthesized generator is controlled by a computer to keep the reed at its resonance frequency f_r. At negligible thermal expansion relative changes of the sound velocity can be measured by the shift of the resonance frequency $\delta f_r/f_r = \delta v/v$. The absolute value of the internal friction Q^{-1} is determined by recording and evaluating resonance curves. In order to measure the variation Q^{-1} it is not necessary to record complete resonance curves at each temperature, but measure the amplitude of the reed A_0, since $Q^{-1} \propto A_0^{-1}$.

The two glasses investigated in this work amorphous GeO_2 and amorphous B_2O_3 are both highly hygroscopic. The a-GeO_2 sample was produced by thermal decomposition under vacuum conditions.[29] An OH^- concentration of about 1% for this sample was determined using the Rutherford-backscattering method.[30] Amorphous B_2O_3 was available with two very different water contaminations, 1.6% (Ref. 31) and 130 ppm.[32] In the following we will refer to these samples as wet and dry a-B_2O_3, respectively.

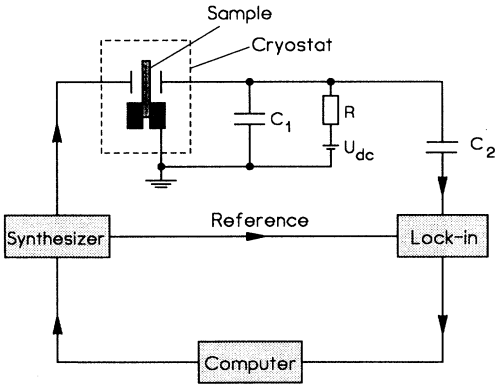

FIG. 3. Experimental setup for the vibrating reed experiments with digitally controlled phase-locked loop. The reed is electrostatically driven by the output of a synthesized generator. The resulting vibration is detected by a lock-in amplifier. To magnify the detected voltage an electrical dc field of about 140 V is applied between the reed and the detection electrode.

IV. EXPERIMENTAL RESULTS

A. a-GeO_2

In Fig. 4 the internal friction of a-GeO_2 at a frequency of 6.3 kHz is shown. At low temperatures it rises with temperature and becomes temperature independent above 200 mK. The initial rise of the absorption is not proportional to T^3 as predicted by Eq. (2.93) of the tunneling model. The reason for it might be a residual absorption of just the right magnitude which cannot be completely avoided. However, in many experiments of this kind an excess absorption was found below 100 mK, following a power law with an exponent between one and two rather than three.[2,8] From the general occurrence of this phenomenon one might conclude that the disagreement of theory and data is fundamental and not just due to the residual absorption. Unfortunately our data are not precise enough to distinguish between these two possibilities. At temperatures between 200 mK and 2 K the internal friction is constant within the errors of our experiment. Using (2.94) we deduce the value $C = 2.45 \times 10^{-4}$ from this plateau.

Above 3 K the internal friction rises linearly with temperature. Such a variation is expected for both relaxation mechanisms, for incoherent tunneling processes [see Eq. (2.94)] and thermally activated processes [see Eq.

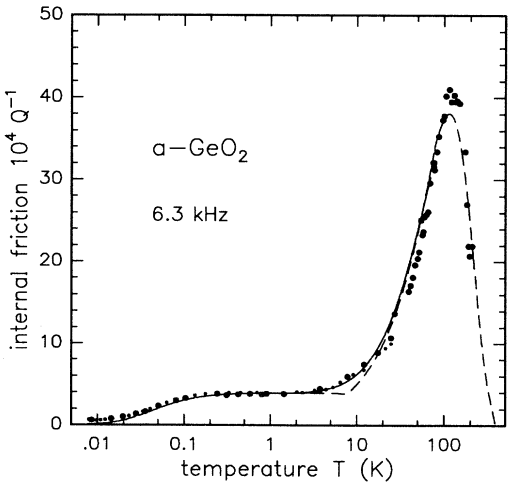

FIG. 4. Internal friction Q^{-1} of a-GeO_2 as a function of temperature. The big dots represent the results of the evaluation of complete resonance curve and the small dots the variation of the reed amplitude. The lines are fits with different theories (see Sec. IV).

(2.103)] as well.

Around 110 K the absorption of a-GeO_2 passes a maximum, which occurs because of the finite width of the distribution $P(V)$ of the barrier heights. Following Tielbürger *et al.*[13] we used the Gaussian distribution eq. (2.102) for the numerical fit of our data. From the frequency dependence of the temperature T_{max} where the maximum occurs, one can find out which of the two relaxation processes is dominant at that temperature. If thermally activated barrier crossing is the dominant process we expect $T_{max} \propto \ln \omega$, whereas incoherent tunneling processes would lead to the relation $T_{max} \propto \sqrt{\omega}$. By comparing our results with measurements at ultrasonic frequencies[33] and Brillouin scattering experiments at 25 GHz,[34] we conclude that thermally activated processes are dominant at the temperature of the maximum.

We have fitted the data in two different ways. In both cases we have taken into account the one-phonon process which dominates at low temperatures. The solid line in Fig. 4 follows from Eq. (2.89), where incoherent tunneling processes are included. This calculation was not continued to temperatures where the absorption peak is observed because the underlying relaxation process there is not dominant anymore. The dashed line was obtained using Eq. (2.97) taking into account thermally activated processes and the distribution function Eq. (2.102), but neglecting incoherent tunneling. The relevant fitting parameters are listed in Table I. Here we want to stress that in the intermediate temperature range from 4 K to 20 K better agreement between theory and experiment is achieved if incoherent tunneling is taken into account, although no additional parameters have been introduced. Therefore we conclude that this process caused the transition from the plateau to the rise at higher temperatures.

The relative change $\delta v/v$ of the sound velocity of a-GeO_2 with temperature is shown in Fig. 5. Between 2 K and 15 K we observed a linear decrease of the velocity with temperature. Using Eq. (2.96) and the same parameters as for the fit of the internal friction we found the solid line. A fit of comparable quality is also provided by Eq. (2.104) based on thermally activated relaxation (not shown in Fig. 5).

The variation of $\delta v/v$ below 1 K is shown in Fig. 6 on a logarithmic scale. In agreement with the tunneling model the velocity first increases logarithmically with temperature due to the resonant interaction. With rising temperature relaxation becomes more and more important leading to a maximum around 80 mK and a subsequent decrease which is proportional to ln T again. The ratio of the ln T slopes in the two regions is nearly $1 : -1$ in contrast to the ratio $2 : -1$ predicted by the tunneling model. Although similar discrepancies have been reported for other glasses,[7] an explanation for this phenomenon is still lacking. Furthermore it is known that the sound velocity of glasses at very low temperature depends on the amplitude of the vibrating reed.[7] We have observed such nonlinearities in our measurements as well. However, all data shown in Fig. 6 where taken at such small driving voltages that the influence of the vibrational amplitude could be neglected even at the lowest temperatures.

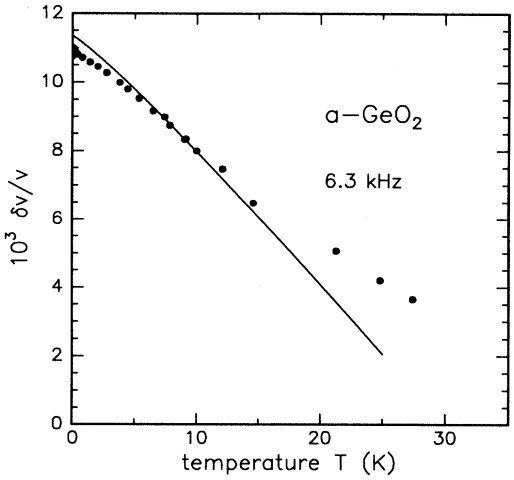

FIG. 5. Relative change of the sound velocity $\delta v/v$ of a-GeO_2. The solid line is a fit according to (2.96).

TABLE I. Parameters of the fits of the GeO_2 data. To determine the deformation potential γ, we have used the mass density $\rho = 3.6$ g/cm^3 and sound velocity $v = 2814$ m/s. The average over the longitudinal and transverse phonon branch is performed via the relations $\gamma^2 \equiv \gamma_\ell^2 = 2\gamma_t^2$ and $v^{-5} = v_\ell^{-5} + v_t^{-5}$.

	Thermal activation	Incoherent tunneling
C	2.45×10^{-4}	2.45×10^{-4}
γ (eV)	1.35	1.35
E_0/k_B (K)	15	—
τ_0 (s)	1.6×10^{-13}	—
$\sigma_0/k_B(K)$	2200	—

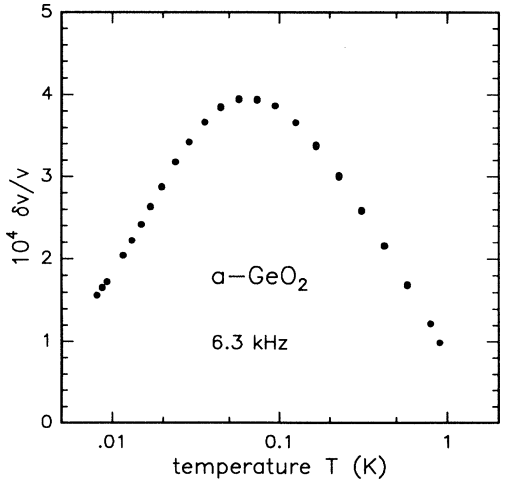

FIG. 6. Relative change of the sound velocity $\delta v/v$ of a-GeO_2 at temperatures below 1 K.

B. a-B_2O_3

The internal friction data of dry and wet a-B_2O_3 are shown in Figs. 7 and 8, respectively. As in the case of a-GeO_2, Q^{-1} first increases with temperature and reaches a temperature independent value of about 5×10^{-4} around $T = 150\,\mathrm{mK}$. At the lowest temperature we again find a significant deviation from the relation $Q^{-1} \propto T^3$ predicted by the tunneling model. It is interesting to note that the internal friction of a-B_2O_3 below 3 K is hardly influenced by the presence of OH^- units.

Above 2 K the absorption of dry a-B_2O_3 increases again and a broad peak is observed. Compared to a-GeO_2 this rise is much less pronounced. The dashed line in Fig. 7 shows that this rise is not well accounted for if incoherent tunneling is neglected and only thermally activated processes are taken into account. It seems to be impossible to improve the agreement as can be seen from Eq. (2.103). Within this model the transition temperature T_a determines the slope of the internal friction at higher temperatures. It is remarkable that again the theory taking incoherent tunneling processes into account yields a much better description of the data in the intermediate temperature range although no free parameter exists. Attempts to fit the results of Fig. 8 for wet a-B_2O_3 lead to the same conclusion. It has to be mentioned that the quality of the fit at very low temperatures could be improved for both sets of data by using a slightly larger deformation potential γ. We will come back to this point in the following section.

Let us now discuss the slope of the absorption peaks. Clearly the acoustic loss is strongly affected by the presence of OH^- impurities. For the dry sample a rather broad peak is observed with its maximum at about 50 K,

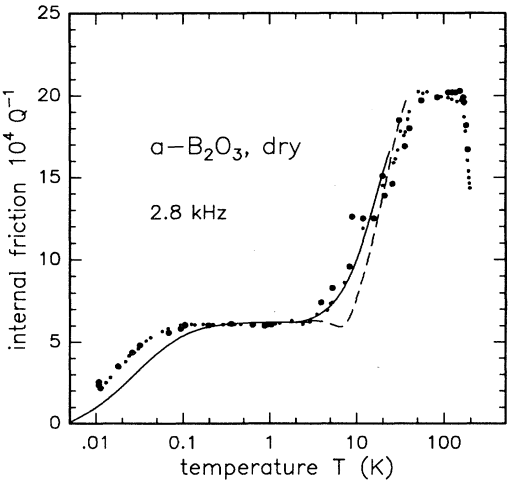

FIG. 7. Internal friction Q^{-1} of dry a-B_2O_3 as a function of temperature. The big dots represent the results of the evaluation of complete resonance curve and the small dots the variation of the reed amplitude. The lines are fits with different theories (see Sec. IV).

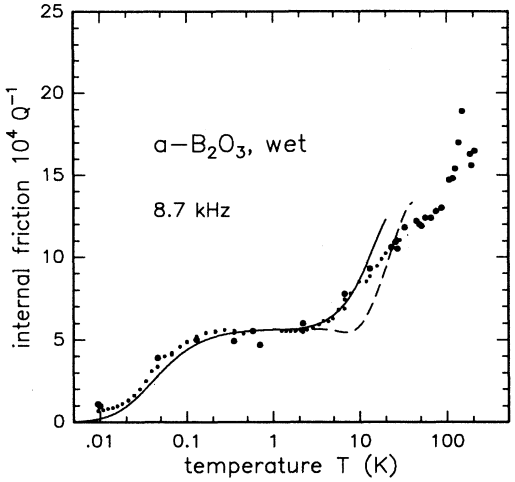

FIG. 8. Internal friction Q^{-1} of wet a-B_2O_3 as a function of temperature. The big dots represent the results of the evaluation of complete resonance curve and the small dots the variation of the reed amplitude. The lines are fits with different theories (see Sec. IV).

while in case of the wet sample we find a shoulder between 30 K and 80 K followed by a narrow peak at about 160 K. These observations are consistent with previous ultrasonic experiments by Kurkijan and Krause[35] on a-B_2O_3 samples with a similar content of OH^- impurities. In those experiments the dry sample exhibited one broad peak whereas the wet one showed two maxima. Having this result in mind we conclude that also in our experiments intrinsic defects cause a loss peak at lower and OH^- impurities a peak at higher temperatures. The superposition of both contributions thus led to experimental curves. In the wet sample the OH^- impurities dominate the absorption behavior and the peak due to intrinsic defects degenerates to a shoulder. Although the OH^- content of the dry sample is lower by 2 orders of magnitude compared to the wet one, it seems to exist still a considerable contribution of OH^- impurities to the observed acoustic loss. Therefore no attempt was made to fit the whole peak as in the case of a-GeO_2 by assuming a Gaussian distribution function for the relevant barrier height. Instead we only show the two theoretical fits of the transition region as discussed above with parameters listed in Tables II and III.

We want to emphasize that the presence of OH^- impurities does not simply lead to two distinct relaxation channels. Obviously the OH^- impurities also change the

TABLE II. Parameters of the fits of the data for dry B_2O_3. To determine the deformation potential γ, we have used $\rho = 1.8\ \mathrm{g/cm^3}$ and $v = 2310\ \mathrm{m/s}$.

	Thermal activation	Incoherent tunneling
C	3.8×10^{-4}	3.8×10^{-4}
γ (eV)	0.65	0.65
E_0/k_B (K)	15	—
τ_0 (s)	$\approx 10^{-13}$	—

TABLE III. Parameters of the fits of the data for wet B_2O_3. To determine the deformation potential γ, we have used $\rho = 1.8$ g/cm^3 and $v = 2373$ m/s.

	Thermal activation	Incoherent tunneling
C	3.6×10^{-4}	3.6×10^{-4}
γ (eV)	0.65	0.65
E_0/k_B (K)	15	—
τ_0 (s)	$\approx 10^{-13}$	—

properties of the intrinsic systems. This can directly be seen from the remarkable fact that the integral absorption of the dry sample is higher than that of the wet sample. This is probably due to structural changes of the amorphous network by the incorporated water. From NMR experiments[36] it is known that the average coordination number of the boron atoms increases with OH^- concentration from 3 to 4.

In Figs. 9 and 10 the temperature dependence of the relative change of the sound velocity of dry and wet a-B_2O_3 is shown. The velocity varies linearly with temperature up to 10 K in the case of the wet sample and up to 20 K for dry a-B_2O_3. Note that the total variation of the sound velocity up to 30 K differs for the two samples by about 40%. The full line in these figures represents a fit using Eq. (2.96) and the parameter of Tables II and III.

Below 1 K the sound velocity of the two samples varies as shown in Figs. 11 and 12. The overall behavior of both samples is very similar to that of a-GeO_2. In the case of the dry sample it was not only possible to carry out measurements at 2.8 kHz, the frequency of the fundamental mode, but also at 16.8 kHz, the frequency of the overtone. Independent of frequency the sound velocity increases logarithmically at the lowest temperature, passes a maximum and decreases logarithmically to higher temperatures. The maximum temperature $\tilde{T}$ follows the relation $\tilde{T} \propto \omega^{1/3}$, in agreement with the tunneling model. A conclusive statement concerning the

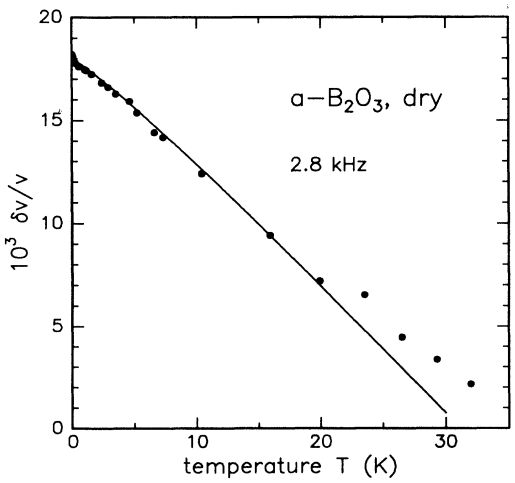

FIG. 9. Relative change of the sound velocity $\delta v/v$ of dry a-B_2O_3. The solid line is a fit according to (2.96).

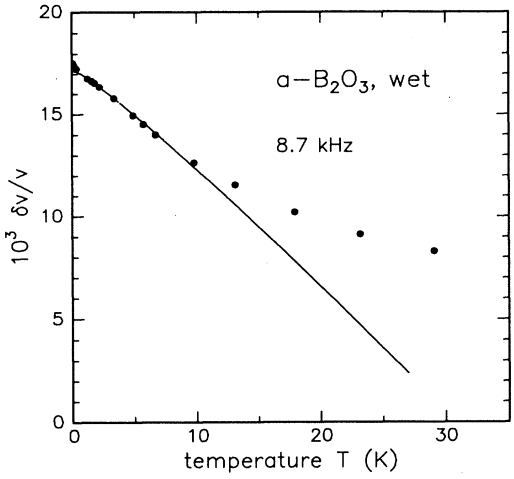

FIG. 10. Relative change of the sound velocity $\delta v/v$ of wet a-B_2O_3. The solid line is a fit according to (2.96).

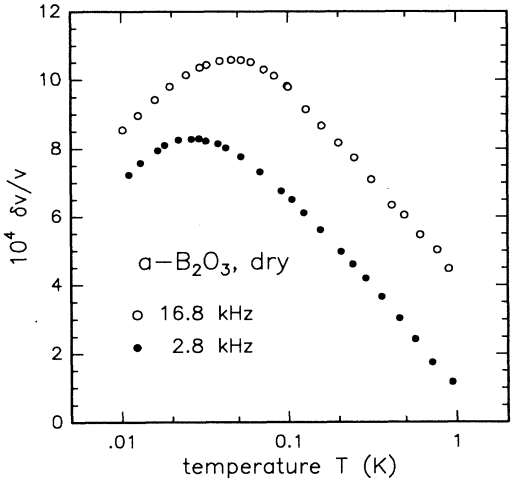

FIG. 11. Relative change of the sound velocity $\delta v/v$ of dry a-B_2O_3 at temperatures below 1 K and at two different frequencies.

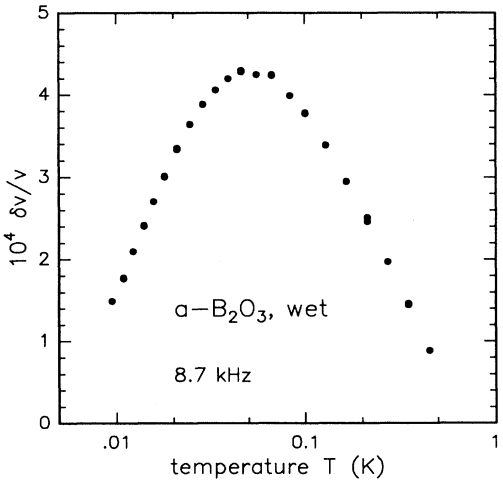

FIG. 12. Relative change of the sound velocity $\delta v/v$ of wet a-B_2O_3 at temperatures below 1 K.

ratio of the slopes below and above the maximum temperature cannot be made because the low temperature range is not wide enough. However, the 16.8 kHz measurement seems to indicate the ratio $1 : -1$. From the data of the wet sample we again deduce the ratio $1 : -1$.

V. SUMMARY

In the previous section we have reported on measurements of the sound propagation in the oxide glasses a-GeO_2 and a-B_2O_3. In both materials the temperature variation of the internal friction is characterized by an increase at lowest temperature followed by a plateau range and finally by a pronounced peak. The sound velocity first rises logarithmically with temperature; after passing through a maximum, it first decreases logarithmically and becomes linear in T at still higher temperature. A similar behavior has been found for other amorphous solids.[2,7]

At low temperatures the acoustic properties of glasses are determined by the interaction with tunneling systems. Depending on frequency and temperature range, sound velocity and internal friction exhibit a behavior which is characteristic for amorphous solids. With respect to the dynamics of the tunneling systems, four regimes are to be distinguished.

(i) *Resonant interaction.* At very low temperatures, i.e., for $T \ll 1\,\mathrm{K}$, the TS's show weakly damped oscillations. The dominant absorption process for sound waves with frequency ω is given by the interaction with TS whose energy splitting fullfils the resonance condition $E = \hbar\omega$. At higher temperatures or low frequencies, $k_B T \gg \hbar\omega$, this process is suppressed, since both levels are equally occupied.

(ii) *Relaxation of asymmetric TS.* At temperatures below 5 K sound attenuation via relaxational absorption occurs because there are TS's satisfying the condition $\omega\tau_1 \approx 1$. Due to the weak damping condition $\widetilde{\Gamma} \ll E$, only asymmetric TS's contribute with an amplitude Δ^2/E^2.

(iii) *Relaxation of overdamped TS's.* Following our discussion of Secs. II A 2 and II A 3, the tunneling oscillations disappear at $k_B T^* = 2/(\pi\widetilde{\gamma})$. For $T > T^*$ the motion of the TS's between the two wells occurs by incoherent tunneling; accordingly the correlation function is that of a Debye relaxator with rate $1/\tau_1$ [cf. Eqs. (2.68) and (2.74)]. Inserting measured values for the parameters yields $T^* \approx 5$ K.

(iv) *Thermally activated relaxation.* At even higher temperature the two-level description becomes invalid. The finite occupation of excited states in the double-well potential results in thermally activated relaxation whose rate can be described by an Arrhenius law $\tau_{\mathrm{th}}^{-1} = \tau_0^{-1} e^{-V/k_B T}$. For τ_{th}^{-1} much larger than the quantum tunneling rate $\widetilde{\Gamma}$, quantum effects have disappeared and the motion in the double-well potential of Fig. 1 can be described by classical mechanics. Because of its dependence on the unknown parameters τ_0 and V, the crossover temperature has to be inferred from experiment.

For $T < 5$ K relaxation of tunneling systems with finite asymmetry and $\omega\tau_1 \approx 1$ appears to be the most effective dissipation mechanism. The relaxation process of biased TS's has been elaborated by Jäckle[6] using Fermi's Golden Rule; in the weak damping limit $\widetilde{\Gamma} \ll E$ corresponding to ranges (i) and (ii), our approach yields results identical to Jäckle's.

At about 5 K, experiments show a significant change in the dynamical behavior of tunneling systems. Obviously the usual description based on a two-state approximation and perturbation theory fails to account for the tunneling dynamics above 5 K; yet it is not clear from the beginning which feature has to be modified in order to properly describe the observed relaxational dynamics.

As mentioned in the Introduction, two physical mechanisms are to be envisaged. Predominance of a thermally activated rate implies the breakdown of the two-level picture [cf. (iv)], whereas incoherent tunneling according to (iii) still relies on the two-state approximation but requires one to go beyond perturbation theory and to apply a strong-coupling theory on the interaction of the tunneling system with phonons.

The mode-coupling approach of Sec. II A 2 yields a qualitative change in the dynamics at a temperature $T^* = 2/k_B\pi\widetilde{\gamma}$; this picture is supported by higher-order terms of the perturbation series which indicate the perturbative approach to be invalid for $T > T^*$. Our mode-coupling theory does not allow for additional parameters; the onset temperature T^* and the slopes of internal friction and sound velocity are determined by the coupling constant $\widetilde{\gamma}$. Thus we are led to ascribe the temperature dependence at $T \geq 5$ K to overdamped two-level systems.

Adjusting only the parameters $\widetilde{\gamma}$ and C, we find surprisingly good agreement of our theory with various experimental quantities: the low-temperature increase of the internal friction, its plateau value, the onset temperature of the increase towards the relaxation peak and the corresponding slope, and the slope of the linear decrease of sound velocity between 1 and about 20 K. The solid lines in Figs. 4–12 are calculated with the parameters listed in the tables.

The results from mode-coupling theory fit the data for both B_2O_3 and GeO_2; a similar agreement has been found for Suprasil W.[19] As a general feature, the calculated onset of the attenuation plateau occurs at too high a temperature; here the agreement could be improved by using a value for the deformation potential γ different from that derived from the high-temperature features.

Because of its much stronger temperature dependence, at some point thermal activation will exceed the quantum tunneling rate, ultimately leading to a classical Arrhenius behavior. The frequency dependence of the maximum of the relaxation peak, $T_{\mathrm{max}} \propto \ln(\omega)$ clearly indicates an activated rate; from this we conclude that at 40 K, most systems are already in the thermally activated regime. (Neglecting thermal activation, the mode-coupling approach would yield a variation of the peak temperature with $\sqrt{\omega}$.)

Clearly, strong TLS-phonon coupling can only be responsible for the experimental findings as long as the concept of long-wavelength Debye phonons is meaningful

in glasses. As linear dispersion of phonons has been observed in amorphous solids up to an experimental threshold of about 400 GHz by Rothenfusser *et al.*,[37] it is proven that Debye phonons exist at least up to temperatures of about 20 K. However, one must note that the relaxation behavior of overdamped TLS's at temperature T is dominated by phonons having frequency $\widetilde{\Gamma}(T)/\hbar > k_B T$, as the E integration in Eqs. (2.89) and (2.90) is cut at $\widetilde{\Gamma}$ for $T > T^*$. From this we can conclude that our model is physically relevant at least up to 10 K. For higher temperatures, one expects that the concept of delocalized undamped phonons smoothly looses its validity. Noting that relaxation phenomena at 20 K demand phonons of about 70 K, the quoted temperature of 20 K might serve as a reasonable order of magnitude where both the two-state approximation and the concept of Debye phonons become invalid.

In Sec. II C we have shown that the strong increase of the internal friction and the linear temperature dependence of sound velocity observed above 5 K can be derived from both incoherent tunneling and thermal activation; yet the mode-coupling theory does not allow for additional parameters and fits the data better than the thermally activated process (see Figs. 4, 7, and 8).

There remains discrepancies at very low temperature for both sound velocity and attenuation. The measured internal friction does not increase as $Q^{-1} \propto T^3$ as expected from Jäckle's theory;[6] one rather finds a power law with an exponent between one and two. Similar results have been reported earlier for coverglass and Suprasil W.[7,8] Very recently, it has been shown that the spectral density (2.3) may comprise a part linear in frequency. Such a term would govern the dynamics at very low temperature; its weaker variation with frequency leads to a linear temperature dependence of the internal friction and thus provides a possible explanation for the frequently observed excess attenuation.[9] As to the sound velocity, the prefactors of the logarithmic laws below and above $\widetilde{T}$ do not obey the ratio $2 : -1$ as expected from (2.96); instead most experiments show a ratio of $1 : -1$.

We finally remark that the anomalous homogeneous linewidth of optical transitions in glasses $\Gamma_{\text{hom}} \propto T^{\alpha}$, $\alpha = 1 - 2$, can consistently be explained in the present framework by incoherent tunneling.[38]

In summary, we find several ranges for the dynamics of tunneling systems in glasses. Below 5 K, the weakly damped coherent oscillations are well described by perturbation theory; as most prominent features we note the logarithmic temperature dependence of sound velocity and the plateau of the internal friction. Above 5 K the thermal motion of the atoms destroys the phase coherence of the two-level systems, thus requiring a strong-coupling theory; our mode-coupling approach provides a quantitatively correct description of the temperature dependence up to a temperature where both the two-state approximation and the concept of Debye phonons ceases to be valid; thermal occupation of excited levels results in an activated rate and ultimately permits a description in terms of classical mechanics and phonons become overdamped.

ACKNOWLEDGMENTS

Helpful discussions with Heinz Horner, Gernot Kasper, and Georg Weiss are gratefully acknowledged. We also would like to thank Robert Weis and Johannes Classen for experimental support. This work has been partly supported by the Deutsche Forschungsgemeinschaft through Grant No. Hu359/3-3.

[1] R. C. Zeller and R. O. Pohl, Phys. Rev. B **4**, 2029 (1971).
[2] S. Hunklinger and W. Arnold, in *Physical Acoustics*, edited by R. N. Thurston and W. P. Mason (Academic Press, New York, 1976), Vol. 12; S. Hunklinger and A. K. Raychaudhuri, in *Progress in Low Temperature Physics*, edited by D. F. Brewer (Elsevier, Amsterdam, 1986), Vol. IX.
[3] P. W. Anderson, B. I. Halperin, and C. Varma, Philos. Mag. **25**, 1 (1972); W. A. Phillips, J. Low. Temp. Phys. **7**, 351 (1972).
[4] L. Piché, R. Maynard, S. Hunklinger, and J. Jäckle, Phys. Rev. Lett. **32**, 1426 (1974).
[5] J. L. Black and P. Fulde, Phys. Rev. Lett. **43**, 453 (1979).
[6] J. Jäckle, Z. Phys. **257**, 212 (1972).
[7] J. Classen, C. Enss, C. Bechinger, G. Weiss, and S. Hunklinger, Ann. Phys. (Leipzig) **3**, 315 (1994).
[8] P. Esquinazi, R. König, and F. Pobell, Z. Phys. B **87**, 305 (1992).
[9] A. Würger, Europhys. Lett. **28**, 597 (1994).
[10] J. T. Krause, J. Appl. Phys. **42**, 3035 (1971); G. Bellessa, C. Lemercier, and D. Caldemaison, Phys. Lett. **62A**, 127 (1977); G. Bellesa, Phys. Rev. Lett. **40**, 1456 (1978).
[11] P. J. Anthony and A. C. Anderson, Phys. Rev. B **20**, 763 (1979).
[12] P. Doussineau, C. Frenois, R. G. Leisure, A. Levelut, and J.-Y. Prieur, J. Phys. (Paris) **41**, 1193 (1980).
[13] D. Tielbürger, R. Merz, R. Ehrenfels, and S. Hunklinger, Phys. Rev. B **45**, 2750 (1992).
[14] F. N. Ignatiev, V. G. Karpov, and M. Klinger, J. Non-Cryst. Solids **55**, 307 (1983).
[15] U. Buchenau, Yu. M. Galperin, V. L. Gurevich, D. A. Parshin, M. A. Ramos, and H. R. Schober, Phys. Rev. B **46**, 2798 (1992).
[16] U. Buchenau, Yu. M. Galperin, V. L. Gurevich, and H. R. Schober, Phys. Rev. B **43**, 5039 (1991).
[17] D. A. Parshin, Phys. Scr. **T49**, 180 (1993).
[18] P. Neu and A. Würger, Z. Phys. B **95**, 385 (1994).
[19] P. Neu and A. Würger, Europhys. Lett. **27**, 457 (1994).
[20] H. Mori, Progr. Theor. Phys. **33**, 127 (1965); R. Zwanzig, J. Chem. Phys. **33**, 1338 (1960).
[21] R. Beck, W. Götze, and P. Prelovsek, Phys. Rev. A **20**, 1140 (1979); W. Zwerger, Z. Phys. B **53**, 53 (1983); **54**, 87 (1983); W. Götze and G. M. Vujicic, Phys. Rev. B **38**, 87 (1988).
[22] P. Neu, Ph.D. thesis, Universität Heidelberg, 1994 (unpublished).
[23] U. Weiss, H. Grabert, and S. Linkwitz, J. Low. Temp. Phys.

68, 213 (1987).

[24] Note that compared to Ref. 19 we have changed the definition of $\tilde{\gamma}$. To get the expression used here, $\tilde{\gamma}$ defined in Ref. 19 must be multiplied by $\pi/\hbar$.

[25] H. A. Kramers, Physica **7**, 284 (1940).

[26] P. Hänggi, P. Talkner, and M. Borkovec, Rev. Mod. Phys. **62**, 251 (1990).

[27] A. J. Leggett, S. Chakravarty, A. T. Dorsey, M. P. A. Fisher, A. Garg, and W. Zwerger, Rev. Mod. Phys. **59**, 1 (1987); U. Weiss, *Quantum Dissipative Dynamics*, Series in Modern Condensed Matter Physics Vol. 2 (World Scientific, Singapore, 1993).

[28] B. S. Berry and W. C. Pritchet, IBM J. Res. Develop. **19**, 334 (1975).

[29] The a-GeO_2 sample was produced by Dr. Schönherr at the Max-Planck Institut für Festkörperforschung in Stuttgart.

[30] These measurements have been performed at the MPI für Kernphysik in Heidelberg. The obtained OH^- concentration can be considered as a upper limit, since the penetration depth of this method is only 0.8 μm. A significantly lower OH^- concentration in the bulk of the sample cannot be excluded.

[31] a-B_2O_3 with 1.6 % OH^- was provided by Professor Quitmann from the Freie Universität Berlin.

[32] Specially dried a-B_2O_3 glass containing about 130 ppm OH^- was produced by Schott Glaswerke in Mainz.

[33] R. E. Strakna and H. T. Savage, J. Appl. Phys. **35**, 1445 (1964).

[34] S. Rau, Ph.D. thesis Universität Heidelberg, 1995 (unpublished).

[35] C. R. Kurkjian and J. T. Krause, J. Am. Ceram. Soc. **49**, 171 (1969).

[36] P. J. Bray, *Interaction of Radiation with Solids* (Plenum, New York, 1970), p. 30.

[37] M. Rothenfusser, W. Dietsche, and H. Kinder, Phys. Rev. B **27**, 5196 (1983); Springer Series in Solid State Sciences Vol. 51, edited by W. Eisenmenger, K. Lassmann, and S. Döttinger (Springer, Berlin, 1984), p. 419.

[38] P. Neu and A. Würger, Europhys. Lett. **29**, 561 (1995).